

Water-Based Dual-Band Metamaterial Absorber

Zhekov, Stanislav Stefanov; Mei, Peng; Fan, Wei; Pedersen, Gert Frølund

Published in:

15th European Conference on Antennas and Propagation, EuCAP 2021

DOI (link to publication from Publisher):

[10.23919/EuCAP51087.2021.9411323](https://doi.org/10.23919/EuCAP51087.2021.9411323)

Publication date:

2021

Document Version

Accepted author manuscript, peer reviewed version

[Link to publication from Aalborg University](#)

Citation for published version (APA):

Zhekov, S. S., Mei, P., Fan, W., & Pedersen, G. F. (2021). Water-Based Dual-Band Metamaterial Absorber. In *15th European Conference on Antennas and Propagation, EuCAP 2021* Article 9411323 IEEE (Institute of Electrical and Electronics Engineers). <https://doi.org/10.23919/EuCAP51087.2021.9411323>

General rights

Copyright and moral rights for the publications made accessible in the public portal are retained by the authors and/or other copyright owners and it is a condition of accessing publications that users recognise and abide by the legal requirements associated with these rights.

- Users may download and print one copy of any publication from the public portal for the purpose of private study or research.
- You may not further distribute the material or use it for any profit-making activity or commercial gain
- You may freely distribute the URL identifying the publication in the public portal -

Take down policy

If you believe that this document breaches copyright please contact us at vbn@aub.aau.dk providing details, and we will remove access to the work immediately and investigate your claim.

Water-Based Dual-Band Metamaterial Absorber

Stanislav Stefanov Zhekov, Peng Mei, Wei Fan, Gert Frølund Pedersen

Department of Electronic Systems, Technical Faculty of IT and Design, Aalborg University, Aalborg, Denmark

e-mail: stz@es.aau.dk; mei@es.aau.dk; wfa@es.aau.dk; gfp@es.aau.dk

Abstract—This paper presents a study on a dual-band metamaterial absorber containing water in the structure. Two designs are considered as each absorber contains metal resonators printed on a substrate, a layer of pure water, a metal ground plane, and a layer of plastic isolating the water from the substrate and the metal plate. The two absorbers differ in the configuration of the used water container. One of the designs demonstrates one absorption peak at high frequency while the other design two peaks when the metal resonators are removed from the structure. The simulated results reveal that the designs have a narrow low and a wide high frequency absorption band. The absorption performance for different temperatures of the water is studied. The temperature change is taken through a change in the dielectric properties of the water. Some reconfiguration of the absorption performance can be achieved by changing the water temperature.

Index Terms—Absorber, dual-band, metamaterial, water.

I. INTRODUCTION

Designing of electromagnetic metamaterial absorbers has been of a large research interest in the past years. This type of absorbing structures are attractive due to their advantages, over traditional microwave absorbers, such as low profile (light weight and small thickness) and easy to install together with antennas to improve the performance of the radiators. The first emergence of a metal-dielectric absorber called “perfect metamaterial absorber” has been presented in [1].

Various designs of unit cells of absorbers based on metamaterials are available in the literature. Polarization-insensitive designs of absorbers have been presented in [2]–[4], [7], [8]. The achievement of such a performance requires the employment of highly symmetrical metal patterns (resonators). Absorbers operating over a wide range of incidence angles have been shown in [2], [7]–[13]. Designs of band-notched absorbers have been presented in [5], [6]. Many efforts have been devoted to designing structures having multi-band absorption [2], [3], [7]–[10], [12]–[15]. Multi-band absorbers are realized by employing multiple metallic resonators with different sizes (i.e. different resonance frequency) arranged in the unit cell. The resonant nature of such a structure, however, makes it quite narrowband. A possibility to expand the absorption bandwidth is by combining the resonances of two or more different structures [10], [12], [16]. The use of matching load for multi-band bandpass frequency selective surface filters is another way to broaden the width of the operation bands [14].

In this paper, two metamaterial absorbers, having a layer of pure water in the structure, are presented. The two unit cells have a difference in the design of the plastic structure

holding the water. The absorbers demonstrate a narrow low and a wide (in the sense of multi-band absorbers) high frequency operation band. It should be mentioned that various designs of water-based metamaterials have already been demonstrated in [17]–[31]. From all these works, however, only in [18] design using metal pattern printed on PCB and having water underneath have been discussed, i.e. configuration similar to ours. However, in [18] wide band absorber (using square patches) has been of interest, while in this paper we study dual-band absorbers (using cross-shaped resonators). How the variation of the water temperature (this changes the value of the complex relative permittivity of the water) affects the absorption response of the studied structures is demonstrated in this paper (similar studies can also be found in the literature). The motivation of the work is to study the opportunity of having absorber with high absorption level over two frequency bands when using pure water as a substrate and whether the good absorption capabilities are preserved when the frequency bands are shifted (thus “extension” of the operation band is achieved) by changing the water temperature. All studies presented in the paper were conducted by using CST Microwave Studio 2020.

II. DESIGN OF THE ABSORBERS

Two absorbers having a layer of pure water were investigated and the geometry of the unit cell of each of them is shown in Fig. 1. The absorbers contain cross-shaped metal resonators (1 large cross controlling the low frequency resonance and 4 small crosses affecting the high frequency resonance), made of copper with conductivity $\sigma = 5.8 \times 10^7$ S/m. The metal patterns are printed on a FR4 substrate with a thickness of 1 mm and having dielectric constant $\epsilon_r' = 4.3$ and loss tangent $\tan(\delta) = 0.025$. In both absorber designs, a plastic layer, with a thickness of 1 mm and with $\epsilon_r' = 2$ and $\tan(\delta) = 0.0002$, is placed underneath the substrate. Then, a layer of pure water, with a thickness of 1 mm, is located. The water layer is isolated from the metal plate, placed at the back of the structure, through another 1 mm thick layer of plastic. The use of a metal ground plane ensures that there is no transmission of signal and the absorption coefficient can be calculated by using only the reflection coefficient of the structure. All geometrical dimensions for the two absorbers are given in Table I. The two unit cells have the same dimensions. The thickness of each metallization in the structure is of 0.035 mm.

The difference between the two designs is in the container keeping the water. In design 1 (Fig. 1(a)), the water is closed from each side with plastic layer, while in design 2 (Fig. 1(b))

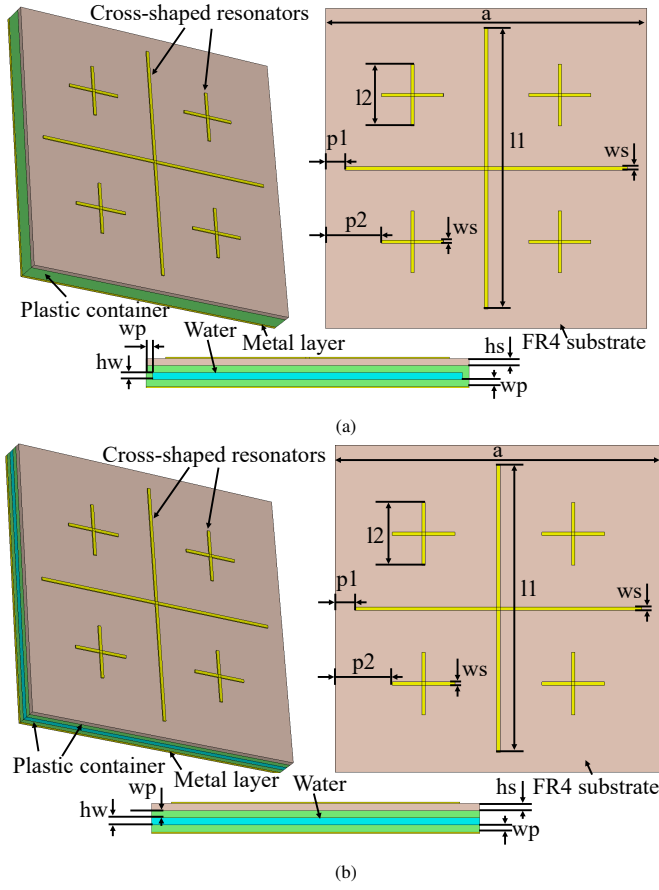


Fig. 1: Geometry of the unit cell of the investigated metamaterial absorbers: (a) design 1, and (b) design 2.

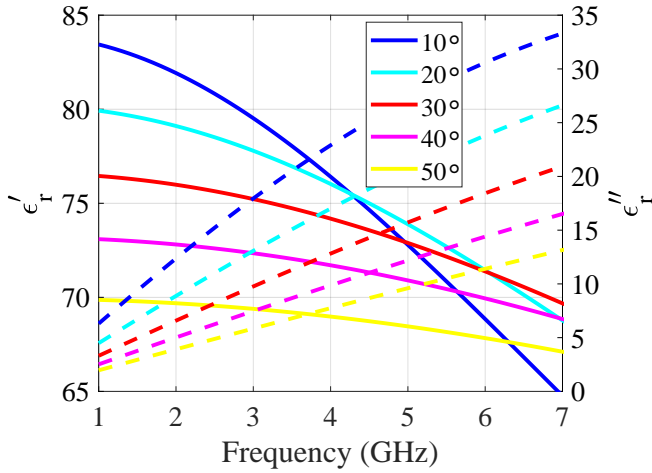


Fig. 2: Dielectric properties of pure water at 10°, 20°, 30°, 40°, and 50° C. The solid lines correspond to the real part ϵ'_r while the dashed lines to the imaginary part ϵ''_r of the complex relative permittivity.

a	hw	wp	hs	ws	$p1$	$p2$	$l1$	$l2$
48	1	1	1	0.5	2.9	12.75	42.2	9.2

TABLE I: Design parameters for the two unit cell absorbers (unit: mm).

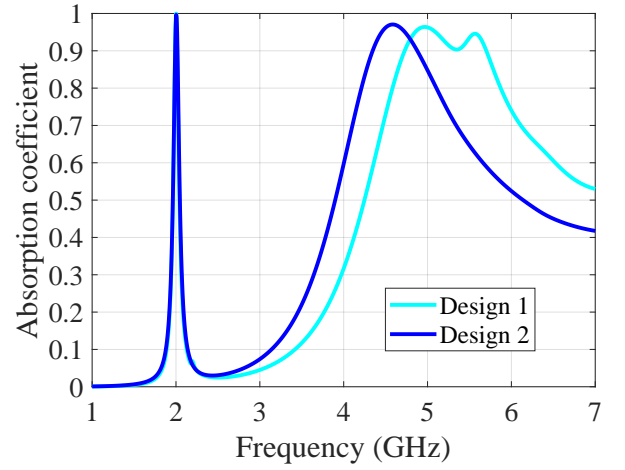


Fig. 3: Absorption coefficient for design 1 and design 2 for pure water at 20° C temperature.

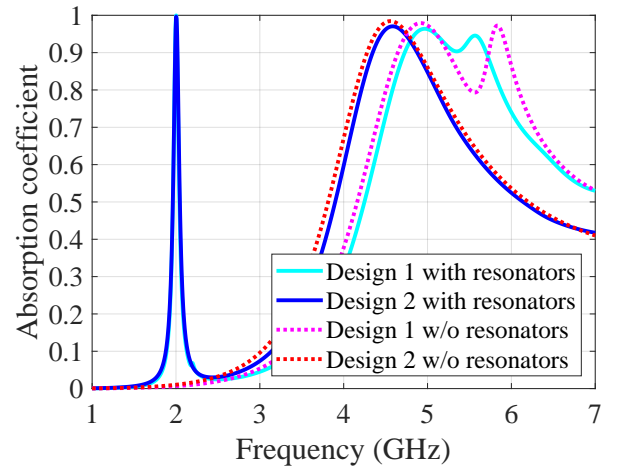
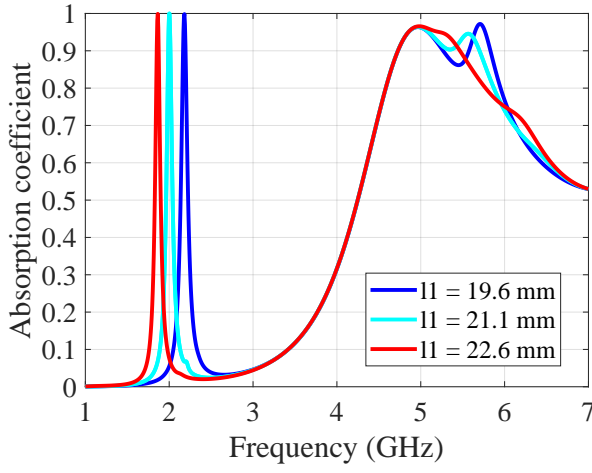


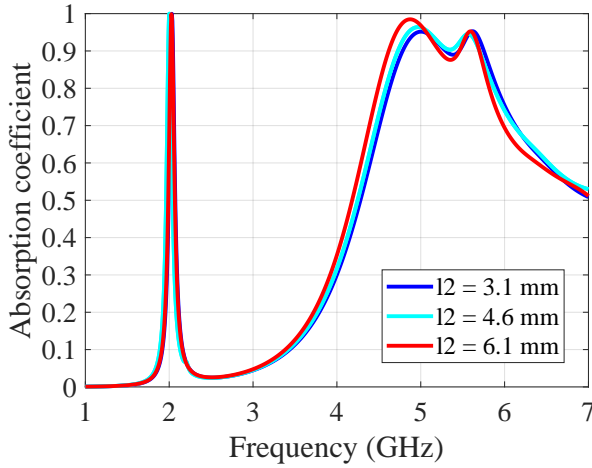
Fig. 4: Absorption coefficient for design 1 and design 2 with (solid lines) and without (dotted lines) resonators for pure water at 20° C temperature.

the water is confined by plastic layer only on the top and bottom. For design 2 is considered that the outermost unit cells along the borders of a final absorber (array of unit cells) will have a plastic wall on the external side, while the unit cells at the corners of the array will have plastic walls on the two external sides. Thus, the water will be hold within the final absorber.

The frequency dependence of the dielectric properties of pure water for temperatures of 10°, 20°, 30°, 40°, and 50° C and at standard atmospheric pressure is shown in Fig. 2. The complex permittivity was obtained by using the Debye model given in [32]. The complex relative permittivity at these five temperatures is presented because the variation of the absorption rate with the temperature is studied in the paper. In all other presented investigations, however, water with a temperature of 20° C is used since this is considered as a normal room temperature.



(a)

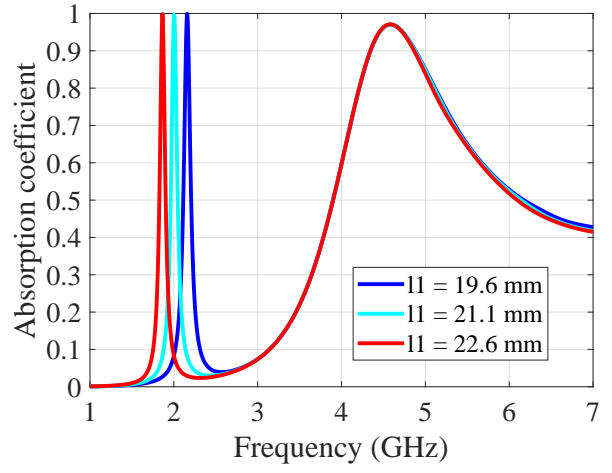


(b)

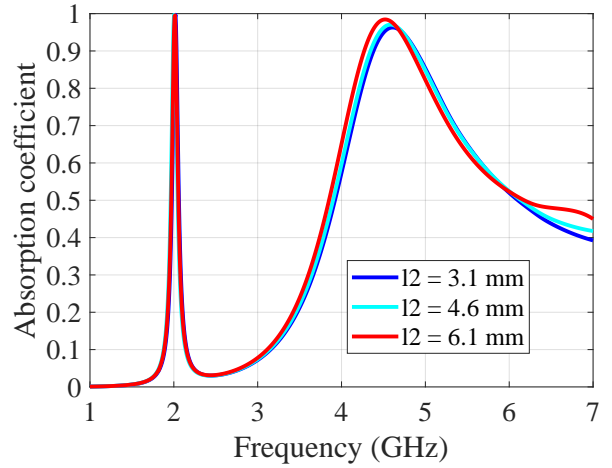
Fig. 5: Absorption coefficient for design 1 for length of: (a) long cross-shaped resonator l_1 of 19.6, 21.1, and 22.6 mm, and (b) short cross-shaped resonators l_2 of 3.1, 4.6, and 6.1 mm.

III. RESULTS

The water has quite different dielectric properties from these of air/vacuum and therefore significantly different impedance. The metamaterial serves as a matching layer between the free space and water. The absorption coefficient for the two designs as a function of frequency is presented in Fig. 3. The results are given only for one of the two linear polarizations since due to the symmetry of the cross-shaped resonators the results for the other linear polarization are the same. Both absorbers demonstrate two operation bands. Comparing the performance of the two absorbers, one can see that the frequency position of their low frequency peaks matches. However, at the high frequency band design 1 shows one while design 2 exhibits two absorption peaks. The two designs have quite different centers of their covered high frequency bands (the only geometrical difference between the two absorbers is in the water container). For the selected geometry and water temperature the covered bands with absorption coefficient



(a)



(b)

Fig. 6: Absorption coefficient for design 2 for length of: (a) long cross-shaped resonator l_1 of 19.6, 21.1, and 22.6 mm, and (b) short cross-shaped resonators l_2 of 3.1, 4.6, and 6.1 mm.

above 0.9 (i.e. at 0.9 level) are: 1) design 1 - 1.988 GHz - 2.015 GHz (relative bandwidth 1.35%) and 4.727 GHz - 5.701 GHz (relative bandwidth 18.68%); and 2) design 2 - 1.990 GHz - 2.018 GHz (relative bandwidth 1.40%) and 4.346 GHz - 4.877 GHz (relative bandwidth 11.51%). According to the data, the designs have narrow low and wide high frequency absorption bandwidth.

The absorption coefficient of design 1 and design 2, when the cross-shaped resonators are removed, is presented in Fig. 4. The low frequency absorption peak disappears when the long cross-shaped resonator is removed. With or without resonators at high frequency design 1 has two peaks and design 2 has one peak. For design 1, the addition of the four short cross-shaped resonators with the selected length of each arm shifts the two high frequency peaks towards each other. In this way, one wider high frequency absorption band, instead of two narrower bands, is achieved. For design 2, the introduction of the short cross-shaped resonators deteriorates slightly the absorption performance in terms of both peak level and width

of the 0.9 (90%) absorption band. However, these resonators are needed to control the position of the absorption peak.

The effect of the change of the length l_1 of the long cross-shaped resonator on the absorption performance of design 1 and designs 2 is shown in Fig. 5 (a) and Fig. 6 (a), respectively. As one can expect, the increase in l_1 leads to shifting of the low frequency absorption peak to the left. However, for design 1 the change in l_1 also affects the high frequency operation band. More precisely, the results show that the increase of l_1 leads to moving of the second high frequency absorption peak towards the first one.

The impact of the variation of the length l_2 of the short cross-shaped resonator on the absorption performance of design 1 and designs 2 is shown in Fig. 5 (b) and Fig. 6 (b), respectively. For design 1, the shifting of the resonances due to the change of l_2 from the optimal selected value of 4.6 mm brings to the transformation from one to two absorption bands (at 0.9 level) at high frequency. For design 2, the difference between the results for $l_2 = 3.1$ mm and $l_2 = 4.6$ mm is quite small; the further increase of l_2 moves the high frequency peak towards lower frequency. This behavior (slight change in the position of the absorption peak) is observed even when the small crosses are removed (not shown). For design 2, the location of the small resonators has a negligible effect on the high frequency absorption band while for design 1 change in the level of absorption (and thus the bandwidth) is observed (not shown).

Fig. 7 and Fig. 8 show the absorption rate of design 1 and design 2, respectively, when the water has temperature of 10°, 20°, 30°, 40°, and 50° C. As one can see, there is a shift in the position of the absorption peaks due to the variation of the dielectric properties of the water with the temperature. At the lowest studied temperature of 10° C, significant reduction in the absorption bandwidth (at 0.9 level) at high frequency is observed. The water temperature can be used for adjustment of the position of the absorption peak, i.e. reconfigurable absorber can be achieved. If the absorption bands for all studied temperatures of the water are combined (the operation bands at different water temperatures overlap partly) then: 1) design 1 covers the bands - 1.988 GHz - 2.060 GHz (relative bandwidth 3.56%) and 4.727 GHz - 5.791 GHz (relative bandwidth 20.23%); and 2) design 2 covers the bands - 1.968 GHz - 2.035 GHz (relative bandwidth 3.35%) and 4.346 GHz - 5.007 GHz (relative bandwidth 14.13%).

IV. CONCLUSION

Two designs of metamaterial absorbers containing a layer of pure water have been presented in this paper. Both designs use the same type of cross-shaped resonators printed on the same type of FR4 substrate. The difference between the two designs is in the plastic container used for holding the water - in one of the designs the water is completely contained within the unit cell, while in the other one the container has no side walls (it is assumed that when the final absorber is manufactured then only the unit cell located along the boundary of the array will have side walls). The designs have a narrow low frequency and

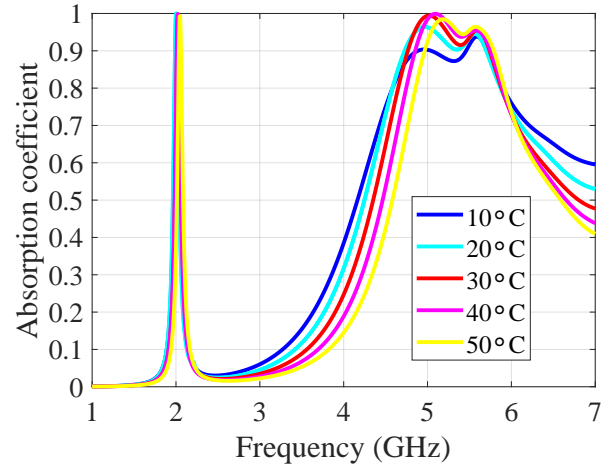


Fig. 7: Absorption coefficient for design 1 for pure water at temperature of 10°, 20°, 30°, 40°, and 50° C.

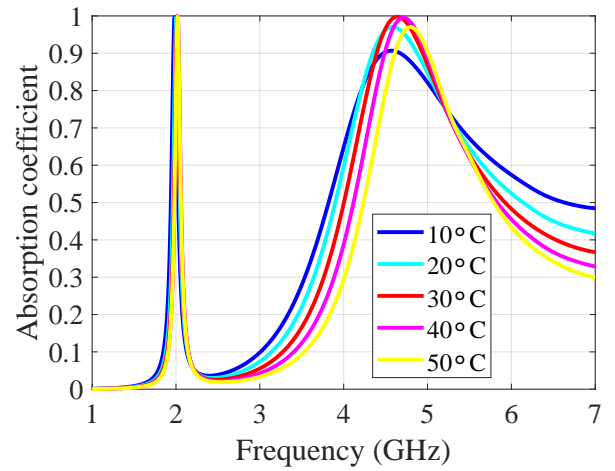


Fig. 8: Absorption coefficient for design 2 for pure water at temperature of 10°, 20°, 30°, 40°, and 50° C.

a wide high frequency operation bandwidth. It has been shown that one of the designs has one absorption peak while the other design two absorption peaks at high frequency when the resonators are not introduced. Design 1 can have two or three absorption bands (depending if it is designed to have one or two operation bands at high frequency), while design 2 has two absorption bands. For design 1, the parametric study has shown that the long and short cross-shaped resonators are coupled to a certain extent while for design 2 they are decoupled. The variation of the dielectric properties of the water with the temperature leads to a change in the performance (absorption peak and bandwidth) of the absorbers. Therefore, tuning of the absorption operation can be achieved just by changing the water temperature.

REFERENCES

- [1] N. I. Landy, S. Sajuyibge, J. J. Mock, D. R. Smith, and W. J. Padilla "Perfect metamaterial absorber," Phys. Rev. Lett., vol. 100, no. 20, 2008.

- [2] Q. Ye, Y. Liu, H. Lin, M. Li, and H. Yang, "Multi-band metamaterial absorber made of multi-gap SRRs structure," *Appl. Phys. A*, vol. 107, no. 1, pp. 155–160, 2012.
- [3] J. Lee and S. Lim, "Bandwidth-enhanced and polarization-insensitive metamaterial absorber using double resonance," *Electron. Lett.*, vol. 47, no. 1, pp. 8–9, 2011.
- [4] S. Ghosh, S. Bhattacharyya, Y. Kaiprath, and K. V. Srivastava, "Bandwidth-enhanced polarization insensitive microwave metamaterial absorber and its equivalent circuit model," *J. Appl. Phys.*, vol. 115, p. 104503, 2014.
- [5] P. Mei, X. Q. Lin, J. W. Yu, A. Boukarkar, P. C. Zhang, and Z. Q. Yang, "Development of a low radar cross section antenna with band-notched absorber," *IEEE Trans. Antennas Propag.*, vol. 66, no. 2, pp. 582–589, Feb. 2018.
- [6] H. Huang, Z. Shen, and A. A. Omar, "3-D Absorptive Frequency Selective Reflector for Antenna Radar Cross Section Reduction," *IEEE Trans. Antennas Propag.*, vol. 65, no. 11, pp. 5908–5917, Nov. 2017.
- [7] D. Chaurasiya, S. Ghosh, and K. V. Srivastava, "Dual band polarization-insensitive wide angle metamaterial absorber for radar application," in *Proc. 44th Eur. Microw. Conf.*, pp. 885–888, 2014.
- [8] N. Mishra, D. K. Choudhary, R. Chowdhury, K. Kumari, and R. K. Chaudhary, "An investigation on compact ultra-thin triple band polarization independent metamaterial absorber for microwave frequency applications," *IEEE Access*, vol. 5, pp. 4370–4376, 2017.
- [9] X. Shen, T. J. Cui, J. Zhao, H. F. Ma, W. X. Jiang, and S. Lim, "Polarization-independent wide-angle triple-band metamaterial absorber," *Opt. Express*, vol. 19, no. 10, pp. 9401–9407, 2011.
- [10] S. Bhattacharyya, S. Ghosh, and K. V. Srivastava, "Triple band polarization-independent metamaterial absorber with bandwidth enhancement at X-band," *J. Appl. Phys.*, vol. 114, p. 094514, 2013.
- [11] O. Luukkonen, F. Costa, C. R. Simovski, A. Monorchio, and S. A. Tretyakov, "A thin electromagnetic absorber for wide incidence angles and both polarizations," *IEEE Trans. Antennas Propag.*, vol. 57, no. 10, pp. 3119–3125, Oct. 2009.
- [12] H. Zhai, C. Zhan, Z. Li, and C. Liang, "A triple-band ultrathin metamaterial absorber with wide-angle and polarization stability," *IEEE Antennas Wireless Propag. Lett.*, vol. 14, pp. 241–244, 2015.
- [13] H. Li, L. H. Yuan, B. Zhou, X. P. Shen, Q. Cheng, and T. J. Cui, "Ultrathin multiband gigahertz metamaterial absorbers," *J. Appl. Phys.*, vol. 110, p. 014909, 2011.
- [14] P. Mei, S. Zhang, X. Q. Lin, and G. F. Pedersen, "A triple-band absorber with wide absorption bandwidths using an impedance matching theory," *IEEE Antennas Wireless Propag. Lett.*, vol. 18, no. 3, pp. 521–525, Mar. 2019.
- [15] H. Luo, Y. Z. Cheng, and R. Z. Gong, "Numerical study of metamaterial absorber and extending absorbance bandwidth based on multi-square patches," *Eur. Phys. J. B*, vol. 81, pp. 387–392, 2011.
- [16] S. Ghosh, S. Bhattacharyya, D. Chaurasiya, and K. V. Srivastava, "An ultrawideband ultrathin metamaterial absorber based on circular split rings," *IEEE Antennas Wireless Propag. Lett.*, vol. 14, pp. 1172–1175, 2015.
- [17] Y. Shen, J. Zhang, Y. Pang, M. Feng, H. Ma, and S. Qu, "Water-based metamaterial absorber for broadband electromagnetic wave absorption," in *Proc. Int. Appl. Comp. Electromagn. Soc. Symp. (ACES)*, pp. 1–2, 2017.
- [18] Y. Pang, J. Wang, Q. Cheng, S. Xia, X. Y. Zhou, Z. Xu, T. J. Cui, and S. Qu, "Thermally tunable water-substrate broadband metamaterial absorbers," *Appl. Phys. Lett.*, vol. 110, p. 104103, 2017.
- [19] Y. J. Yoo, S. Ju, S. Y. Park, Y. J. Kim, J. Bong, T. Lim, K. W. Kim, J. Y. Rhee, and Y. Lee, "Metamaterial absorber for electromagnetic waves in periodic water droplets," *Sci. Rep.*, vol. 5, p. 14018, 2015.
- [20] A. Andryieuski, S. M. Kuznetsova, S. V. Zhukovsky, Y. S. Kivshar, and A. V. Lavrinenko, "Water: promising opportunities for tunable all-dielectric electromagnetic metamaterials," *Sci. Rep.*, vol. 5, p. 13535, 2015.
- [21] M. Odit, P. Kapitanova, A. Andryieuski, P. Belov, and A. V. Lavrinenko, "Experimental demonstration of water based tunable metasurface," *Appl. Phys. Lett.*, vol. 109, p. 011901, 2016.
- [22] Y. Zhou, Z. Shen, X. Huang, J. Wu, Y. Li, S. Huang, and H. Yang, "Ultra-wideband water-based metamaterial absorber with temperature insensitivity," *Phys. Lett. A*, vol. 383, no. 23, pp. 2739–2743, 2019.
- [23] P. J. Bradley, M. O. M. Torrico, C. Brennan, and Y. Hao, "Printable all-dielectric water-based absorber," *Sci. Rep.*, vol. 8, p. 14490, 2018.
- [24] F. S. Santos and V. F. Rodriguez-Esquerre, "Water-based broadband metamaterial absorbers operating at microwave frequencies," in *Proc. Metamaterials, Metadevices, and Metasystems*, p. 114602G, 2020.
- [25] J. Ren, and J. Y. Yin, "Cylindrical-water-resonator-based ultra-broadband microwave absorber," *Opt. Mat. Express*, vol. 8, pp. 2060–2071, 2018.
- [26] Y. Pang, Y. Shen, Y. Li, J. Wang, Z. Hu, and S. Qu, "Water-based metamaterial absorbers for optical transparency and broad band microwave absorption," *J. Appl. Phys.*, vol. 123, p. 155106, 2018.
- [27] X. Huang, H. Yang, Z. Shen, J. Chen, H. Lin, and Z. Yu, "Water-injected all-dielectric ultra-wideband and prominent oblique incidence metamaterial absorber in microwave regime," *J. Phys. D: Appl. Phys.*, vol. 50, 2017.
- [28] J. Zhao, S. Wei, C. Wang, K. Chen, B. Zhu, T. Jiang, and Y. Feng, "Broadband microwave absorption utilizing water-based metamaterial structures," *Opt. Express*, vol. 26, no. 7, pp. 8522–8531, 2018.
- [29] Z. Wu, X. Chen, Z. Zhang, L. Heng, S. Wang, and Y. Zou, "Design and optimization of a flexible water-based microwave absorbing metamaterial," *Appl. Phys. Express*, vol. 12, p. 057003, 2019.
- [30] J. Xie, W. Zhu, I. D. Rukhlenko, F. Xiao, C. He, J. Geng, X. Liang, R. Jin, and M. Premaratne, "Water metamaterial for ultra-broadband and wide-angle absorption," *Opt. Express*, vol. 26, no. 4, pp. 5052–5059, 2018.
- [31] I. V. Stenishchev and A. A. Basharin, "Toroidal response in all-dielectric metamaterials based on water," *Sci. Rep.*, vol. 7, p. 9468, 2017.
- [32] W. J. Ellison, "Permittivity of pure water, at standard atmospheric pressure, over the frequency Range 0–25 THz and the temperature range 0–100 °C," *J. Phys. Chem. Ref. Data*, vol. 36, no. 1, pp. 1–18, 2007.